Full paper / Mémoire

On the protonation of ruthenium-PTA complexes in water. X-ray crystal structure of RuCl$_4$(PTAH)$_2$·4 H$_2$O (PTA = 1,3,5-triaza-7-phosphaadamantane)

Dina N. Akbayeva, Simonetta Moneti, Maurizio Peruzzini, Luca Gonsalvi *, Andrea Ienco, Francesco Vizza *

Consiglio Nazionale delle Ricerche, Istituto di Chimica del Composti Organometallici (CNR–ICCOM), Via Madonna del Piano, snc, 50019 Sesto Fiorentino, Firenze, Italy

Abstract

The X-ray structure of the neutral RuCl$_4$(PTAH)$_2$·4H$_2$O complex containing the *N*-protonated ligand PTAH (PTA = 1,3,5-triaza-7-phosphaadamantane) is presented. The protonated nitrogen atom of PTA forms strong hydrogen bonding with a water molecule, while another water acts as donor to an unprotonated nitrogen atom. The molecular structure of the neutral complex is compared with the cationic Ru(III) analogue previously described. It is shown that removing one electron from the HOMO practically alters neither the Ru–Cl and Ru–P distances nor the values of the angles around the metal atom. ***To cite this article: D.N. Akbayeva et al., C. R. Chimie 8 (2005)***.

Résumé

L'analyse rayon-X du complexe neutre RuCl$_4$(PTAH)$_2$·4H$_2$O contenant le ligand PTAH (PTA = 1,3,5-triaza-7-phosphaadamantane) avec un atome d'azote protoné est présentée ici. L'atome d'azote protoné établit une forte liaison hydrogène avec une molécule d'eau, tandis qu'une autre molécule d'eau agit en tant que donneur pour un atome d'azote non protoné. Le structure moléculaire du complexe neutre a été comparée avec un complexe analogue de Ru(III), déjà décrit. Il est montré que le fait d'enlever un électron de la HOMO n'affecte, ni la longueur de la liaison Ru–Cl ou Ru–P, ni les valeurs des angles autour de l'atome métallique. ***Pour citer cet article : D.N. Akbayeva et al., C. R. Chimie 8 (2005)***.

* Corresponding authors.

*E-mail address:* francesco.vizza@iccom.cnr.it (F. Vizza).

1. Introduction

The water soluble cage adamantane-like phosphine, 1,3,5-triaza-7-phosphaadamantane (PTA, **1**) first reported in 1974 by Daigle et al. [1] has received renewed interest for application in homogeneous aqueous biphasic catalysis and to obtain biologically active transition metal compounds and luminescent gold complexes, together with its *N*-protonated or *N*-alkylated derivatives PTAH and PTA(R), depicted in Scheme 1. All these aspects have been recently reviewed [2].

A unique feature of PTA is the ability to be regioselectively protonated at nitrogen rather than at the phosphorus centre. In water solutions with a pH lower than 6.5, PTA forms the *N*-protonated phosphine PTAH (**2**). The basicity of PTA has been measured with a pK_a of 5.70 [3]. A number of PTAH complexes of various transition metals have been characterised crystallographically, often showing hydrogen bonding through the protonated nitrogen with or without the presence of water molecules [2]. Hereby we report the synthesis and the X-ray crystal structure of $RuCl_4(PTAH)_2 \cdot 4 H_2O$ (**3**). The 3D architecture created by the hydrogen bonding network differs remarkably from the Ru(III) analogue $[RuCl_4(PTAH)_2]Cl \cdot 4 H_2O$ and is here described.

2. Results and discussion

The reaction of excess PTA with hydrated $RuCl_3$ in refluxing ethanol to obtain *cis*-$RuCl_2(PTA)_4$ has been described in Refs. [4,5]. The authors reported that when this compound is reacted with an aqueous HCl solution, the *bis*-protonated species $[RuCl_2(PTA)_2(PTAH)_2]Cl_2$ (**4**) is obtained along with a small amount of Ru(III) complex $[RuCl_4(PTAH)_2]Cl$ (**5**) which was characterised crystallographically (Scheme 2).

However, we found that when the crude product from the first reaction is recrystallised from water solutions after 2 weeks standing on air, black crystals of $RuCl_4(PTAH)_2 \cdot 4 H_2O$ (**3**) suitable for X-ray data col-
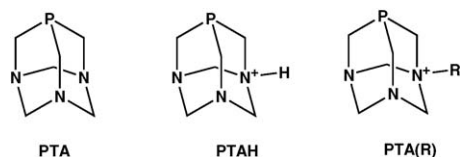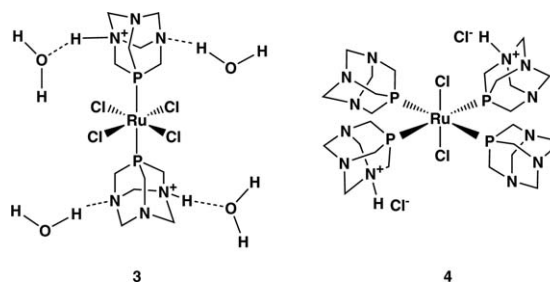
Scheme 2.

lection could be instead recovered. An ORTEP plot of the molecule is shown in Fig. 1. Selected bond distances (Å) and angles (°) are listed in Table 1.

The structure of **3** consists of slightly distorted octahedral molecules of the ruthenium complex and clathrated water molecules in the 1:4 ratio. The two P-bonded phosphine ligands are *trans* to each other in apical position with respect to the equatorial plane identified by the Ru and the four chlorine atoms. The metal atom lies on an inversion centre, thus only one PTAH ligand and two chlorine atoms are present in the asymmetric unit. The protonated nature of the phosphine ligand is consistent with the presence of four coordinated Cl anions, hence the diamagnetic nature of the Ru(II) cen-
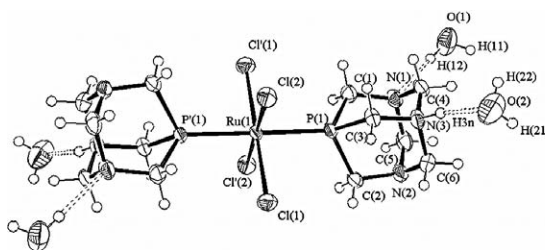
Scheme 1.

Fig. 1. ORTEP diagram for $RuCl_4(PTAH)_2 \cdot 4 (H_2O)$. The symmetry transformations used to generate equivalent atoms is –*x*, –*y*, –*z*.

Table 1
Selected bond lengths (Å) and angles (°) for $RuCl_4(PTAH)_2 \cdot 4 (H_2O)$

Ru(1)–P(1)	2.3417(9)	P(1)–Ru(1)–Cl(1)	88.56(4)
Ru(1)–Cl(1)	2.3622(10)	P(1)–Ru(1)–Cl(1)#1	91.44(4)
Ru(1)–Cl(2)	2.3697(10)	P(1)#1–Ru(1)–Cl(2)	87.36(4)
P(1)–C(1)	1.834(3)	P(1)–Ru(1)–Cl(2)	92.64(4)
P(1)–C(3)	1.838(3)	Cl(1)–Ru(1)–Cl(2)	89.42(3)
P(1)–C(2)	1.839(3)	Cl(1)–Ru(1)–Cl(2)#1	90.58(3)
		C(1)–P(1)–Ru(1)	119.41(9)
		C(3)–P(1)–Ru(1)	119.32(9)
		C(2)–P(1)–Ru(1)	117.61(9)

Symmetry transformations used to generate equivalent atoms: #1 –*x*, –*y*, –*z*.

tre, as confirmed in solution by the appearance of a ^{31}P NMR singlet at –56.2 ppm.

PTAH complexes are also known to form strong intra- and intermolecular $NH^+ \cdots N$ hydrogen bonding and interactions with water molecules interspersed in the lattice. In **3**, two independent water molecules are present in the unit cell with each kind of molecule taking a precise role in supporting the network of hydrogen bonding interactions responsible for the 3D architecture. In this regard, the water molecule belonging to the O(2) atom shows three short contact interactions with neighbouring nuclei forming a strong hydrogen bond with the protonated N(3) atom, with N(3)···O(2) distance at 2.740(4) Å, and establishing hydrogen bonds with symmetry repeated O(2) atoms $(O(2)\cdots O(2)^I$ I = +x, −y + 1/2, +z + 1/2) and with the O(1) oxygen of the second water $(O(2)\cdots O(1)^{II}$ II= −x + 2, −y, −z + 1). The unprotonated nitrogen N(1) interacts also with the second water molecule through the H(12) hydrogen, as shown by the O(1)···N(1) distance at 2.982(4) Å. The other water hydrogen H(11) bonded to O(1) has short contacts with two chlorine atoms of another molecule of $RuCl_4(PTAH)_2$ complex $(O(1)\cdots Cl(1)^{III}$ and $O(1)\cdots Cl(2)^{III}$ III= −x + 1, +y + 1/2, −z + 1/2). The net-

work of hydrogen bonding interactions propping up the solid state structure of **3** is shown in Fig. 2.

$[RuCl_4(PTAH)_2]Cl\cdot 2\ H_2O$ (**5**), i.e. the oxidised Ru(III) analogue of **3** was previously described by Darensbourg et al. [3]. The main differences between the two ruthenium complexes, **3** and **5**, consist in the presence of an extra chlorine atom in the asymmetric unit of the latter and in the different role of the solvated water molecules. These aspects account for the cationic nature of the octahedral Ru(III) species, and for the deep change in the hydrogen bonding network supporting the solid state structure of the two related complexes. The packing diagrams of **3** and **5** are highlighted in Figs. 2 and 3, respectively.

The complex units of **3** are orthogonal to each other while in **5** they are parallel to each other. In the latter structure, the water oxygen O(1) is a hydrogen bond acceptor of the N-protonated PTAH, whereas the remaining N atoms are not involved in hydrogen bonding. Furthermore, the same water is involved in networking with itself in the other layers and with another kind of water molecule, identified by O(2), which in turn has short contacts with Cl(3) on the special position and one of the Ru-coordinated chlorine atoms.
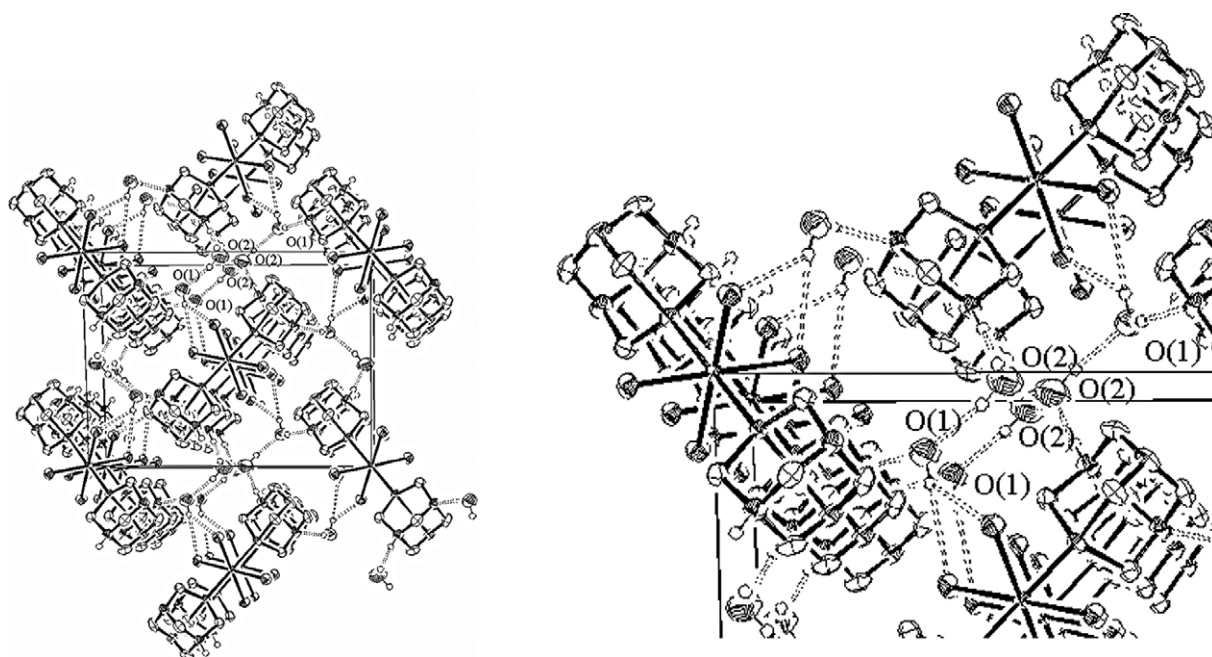

Fig. 2. On the left, packing diagram for $RuCl_4(PTAH)_2\cdot 4(H_2O)$ (view down to the crystallographic axis *a*). For sake of clarity, the hydrogen atoms bonded to carbon atoms were omitted. On the right, blow-up of the hydrogen bonding network.
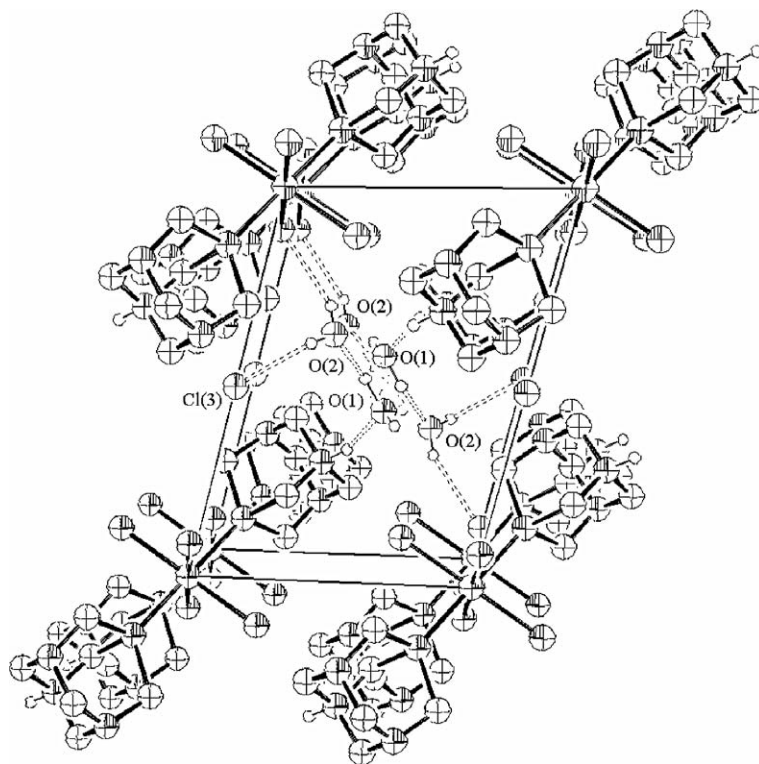
Fig. 3. Packing diagram for RuCl$_4$(PTAH)$_2$$^+$ Cl$^-$ 4 (H$_2$O) (view down to the crystallographic axis *a*). For sake of clarity, the hydrogen atoms bonded to carbon atoms were omitted. Adapted from [4].

An inspection of the bond distances and angles of both complexes indicates that the two ruthenium derivatives share the same geometry around the metal centre and exhibit almost identical metrical parameters, pointing out that the one electron oxidation of the metal atom formally transforming **3** into **5** does not influence the overall geometry of the complex. In keeping with this finding, a semiempirical MO calculation carried out at the Extended Hückel level, suggests that the HOMO of **3** is a non-bonding orbital originating from the 't_{2g}' set of an idealised octahedral symmetry being essentially formed by the d_{xy} atomic orbital slightly perturbed by minor contributions from the p lone pairs of the chlorine atoms. The EHMO calculation on a model of **3**, indicates also that the value overlap population for the Ru–Cl bonds of the oxidised complex is greater than neutral one (0.30 vs. 0.25, respectively) [6].

3. Conclusions

In summary, we have shown that, irrespective of the oxidation state of the metal, the 3D architectures in the solid state structures of RuCl$_4$(PTAH)$_2$·4 H$_2$O is mainly governed by the network of hydrogen bonding interactions formed with water molecules and the N-protonated ligand.

4. Experimental section

PTA was prepared as described in [1]. The ^{1}H and ^{31}P{^{1}H} NMR spectrum of **3** were recorded on Bruker AC200 spectromer operating at 200.13 and 81.01 MHz, respectively. Peak positions are relative to external tetramethylsilane (^{1}H) or measured relative to external 85% H$_3$PO$_4$, with downfield shifts considered positive. Elemental analyses (C, H) were performed using a Carlo Erba model 1106 elemental analyser by the Microanalytical Service of the Department of Chemistry at the University of Florence.

4.1. Synthesis of RuCl$_4$(PTAH)$_2$·4 H$_2$O (**3**)

Solid PTA (2.5 g, 16 mmol) was added under stirring to a solution of RuCl$_3$·3H$_2$O (1.0 g, 4 mmol) in

ethanol (100 ml). The resulting mixture was refluxed for 3 h in the air. During this time the colour of the solution changed from reddish brown to yellowish brown. Cooling the solution to room temperature, and slow concentration in the air gave the crude product as a yellow–brown powder which was filtered off, and washed with ethanol (2 × 10 ml) and pentane (3 × 5 ml) before being dried under a stream of nitrogen (yield 2.5 g). The crude product was dissolved in H_2O (30 ml) and, after 2 weeks, well-formed black crystals of **3** precipitated. They were collected by filtration and washed with ethanol and pentane. Yield (0.5 g, 24%). $^{31}P\{^1H\}$ NMR (81.01 MHz, DMF-d_7 25 °C): δ –56,2, s. ^1H NMR (200.13 MHz, DMF-d_7, 25 °C): δ 4.5–4.7 (m, 6H, NCH_2N), 4.1–4.3 (m, 6H, PCH_2N). Anal. Calcd. for $C_{12}H_{26}N_6Cl_4P_2Ru\cdot4\,H_2O$: C 23.12, H 4.10, N 13.49%. Found: C 23.70, H 4.72, N 13.80%. Addition of ethanol (10 ml) to the mother liquor led to a yellow microcrystalline precipitate of $Ru(PTA)_4Cl_2$ (yield 1.8 g) [4].

4.2. X-ray data collection of $RuCl_4(PTAH)_2\cdot4H_2O$ (3)

A summary of the crystal and refinement data are given in Table 2. Well-formed black crystals of **3** were mounted on an Enraf-Nonius CAD4 diffractometer equipped with a graphite monochromator and Mo–Kα radiation (λ = 0.71073 Å). The cell dimensions were refined by least-squares refinement of 25 reflections in the 2θ range of 10–20°. The intensity data were corrected for Lorentz and polarisation effects and for absorption by means of ψ scan. Three standard reflections were monitored every 2 h during data collection and minimum decay was observed. Atomic scattering factors are those reported by Cromer and Waber [7]. Structure solutions were carried out by direct methods using the SIR-97 package of programs [8]. Refinements were made by full-matrix least-squares on all F^2 data using SHELXL-97 [9]. The anisotropic model was used for the non-hydrogen atoms. The hydrogen atoms bound to carbon were introduced at calculated positions in the later stages of refinement, while those of the water molecules and the one bonded to N(3) were found from ΔF maps. The H atoms bound to carbon atoms were treated with the riding model, however, the N(3)–H distance was constrained to the value of 0.92 Å and the H–O were constrained to the value of 0.82 Å. No unusual trend in ΔF vs. Fo or $(\sin\theta)/\lambda$ was observed.

Table 2

Crystal data and structure refinement for $RuCl_4(PTAH)_2\cdot4\,H_2O$

Empirical formula	$C_{12}H_{34}Cl_4N_6O_4P_2Ru$
Formula weight	631.26
Crystal system	Monoclinic
Space group	$P2_1/c$
Unit cell dimensions	a = 7.193(5) Å, α = 90°
	b = 15.155(5) Å,
	β = 103.715(5)°
	c = 11.420(5) Å, γ = 90°
Volume	1209.4(11) Å^3
Z	2
Density (calculated)	1.733 Mg m^{-3}
Absorption coefficient	1.253 mm^{-1}
$F(000)$	644
Reflections collected	2240
Number of parameters refined	171
Independent reflections	2128 [R(int) = 0.0281]
Absorption correction	Psi-scan
Maximum and minimum transmission	0.7945 and 0.7333
Goodness-of-fit on F^2	1.076
Final R indices [$I > 2\text{sigma}(I)$]	R_1 = 0.0234,
	wR_2 = 0.0631
R indices (all data)	R_1 = 0.0279,
	wR_2 = 0.0660

Final difference syntheses showed no significant electron density residues. The molecular drawings were made using the program ORTEP-III for Windows [10]. All the computational work was performed by using the WINGX package [11]. Supplementary crystallographic data (CCDC 237764) can be obtained free of charge via www.ccdc.cam.ac.uk/data_request/cif, by emailing data_request@ccdc.cam.ac.uk, or by contacting The Cambridge Crystallographic Data Centre, 12, Union Road, Cambridge CB2 1EZ, UK; fax: +44 1223 336 033.

References

[1] (a) D.J. Daigle, A.B. Pepperman Jr., S.L. Vail, J. Heterocycl. Chem. 11 (1974) 407. (b) D.J. Daigle, Inorg. Synth. 32 (1998) 40.

[2] A.D. Phillips, L. Gonsalvi, A. Romerosa, F. Vizza, M. Peruzzini, Coord. Chem. Rev. 248 (2004) 955.

[3] D.J. Darensbourg, T.J. Decuir, J.H. Reibenspies, I.T. Horvath, F. Joó, in: Aqueous Organometallic Chemistry and Catalysis, Kluwer, Dordrecht, The Netherlands, 1995, pp. 61–80.

[4] D.J. Darensbourg, F. Joó, M. Kannisto, A. Katho, J.H. Reibenspies, D.J. Daigle, Inorg. Chem. 33 (1994) 200.

[5] D.J. Darensbourg, F. Joó, M. Kannisto, A. Katho, J.H. Reibenspies, Organometallics 11 (1992) 1990.

[6] (a) R. Hoffmann, W.N. Lipscomb, J. Chem. Phys. 36 (1962) 2872. (b) R. Hoffmann, W.N. Lipscomb, J. Chem. Phys. 37 (1962) 3489.

[7] D.T. Cromer, J.T. Waber, Acta Crystallogr. 18 (1965) 104.

[8] SIR97, A. Altomare, M.C. Burla, M. Cavalli, G.L. Cascarano, C. Giacovazzo, A. Gagliardi, A.G.G. Moliterni, G. Polidori, R. Spagna, J. Appl. Crystallogr. 32 (1999) 115.

[9] SHELXL-97, (crystal structure refinement), University of Göttingen, Germany, 1997.

[10] a) ORTEP-III, M.N. Burnett, C.K. Johnson, Report ORNL-6895. Oak Ridge National Laboratory, Oak Ridge, TN, 1996. b) L.J. Farrugia, J. Appl. Chem. 30 (1997) 565.

[11] L.J. Farrugia, J. Appl. Chem. 32 (1999) 837.